

Monomer Dependence of Colorless and Transparent Polyimide Films: Thermomechanical Properties, Optical Transparency, and Solubility

Yeji Na, Sungsoo Kang, Lee Ku Kwac, Hong Gun Kim, and Jin-Hae Chang*

Cite This: *ACS Omega* 2024, 9, 12195–12203

Read Online

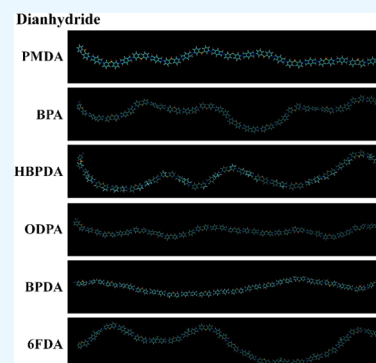
ACCESS |

Metrics & More

Article Recommendations

Supporting Information

ABSTRACT: Six poly(amic acid)s (PAAs) were synthesized by reacting bis(3-amino-phenyl) sulfone with various dianhydride monomers such as pyromellitic dianhydride, 4,4'-biphenyl dianhydride, dicyclohexyl-3,4,3',4'-tetracarboxylic dianhydride, 4,4'-oxidiphthalic anhydride, 3,3',4,4'-benzophenonetetracarboxylic dianhydride, and 4,4'-(hexafluoroisopropylidene) diphthalic anhydride. These PAAs were then converted to polyimide (PI) films by thermal imidization at various temperatures. To obtain colorless and transparent PI (CPI), the dianhydride monomer used in this study had an overall bent structure, a structure containing a strong electron-withdrawing $-\text{CF}_3$ substituent or an alicyclic ring. In addition, some monomers contained ether or ketone functional groups in their bent structures. The thermomechanical properties, optical transparency, and solubility of CPI films with six different dianhydride monomer structures were investigated, and the correlation between the monomer structure and CPI film properties was clarified. Overall, CPI with an aromatic main chain structure or a linear structure had excellent thermal and mechanical properties. In contrast, CPI with a bent structure containing functional groups or substituents in the main chain exhibited excellent optical transparency and solubility.



1. INTRODUCTION

Aromatic polyimide (PI) has a rigid chain structure and excellent thermomechanical properties, chemical resistance, electrical properties, and dimensional stability.^{1–4} Therefore, PI is widely used in aerospace, machinery/automotive, and electrical/electronic materials.^{5–8} However, the rigid rod-shaped linear aromatic structures in which the PI main chain promotes charge transfer-complex (CT-complex) formation exhibit a dark brown color due to intermolecular or intramolecular interactions resulting from the movement of π electrons between polymer chains.^{9,10} For this reason, practical difficulties exist in applying PI to display fields that require colorless and transparent optical properties.

There are several methods to prevent CT-complex formation and synthesize colorless and transparent PI (CPI):^{11–13} (1) inserting a bent monomer into the main chain to reduce the linearity of the main chain structure and limit the movement of π electrons; (2) introducing substituents into the main chain to prevent molecular packing; (3) limiting the movement of π electrons by introducing strong electron-withdrawing groups such as highly electronegative trifluoromethyl ($-\text{CF}_3$) or sulfone ($-\text{SO}_2-$) groups; (4) forming a relatively flexible structure by introducing a free-rotating ether ($-\text{O}-$) group into the main chain; (5) using an alicyclic monomer with no π electron movement in the main chain. Additionally, cycloaliphatic CPI exhibits excellent solubility, a low dielectric constant, and high optical trans-

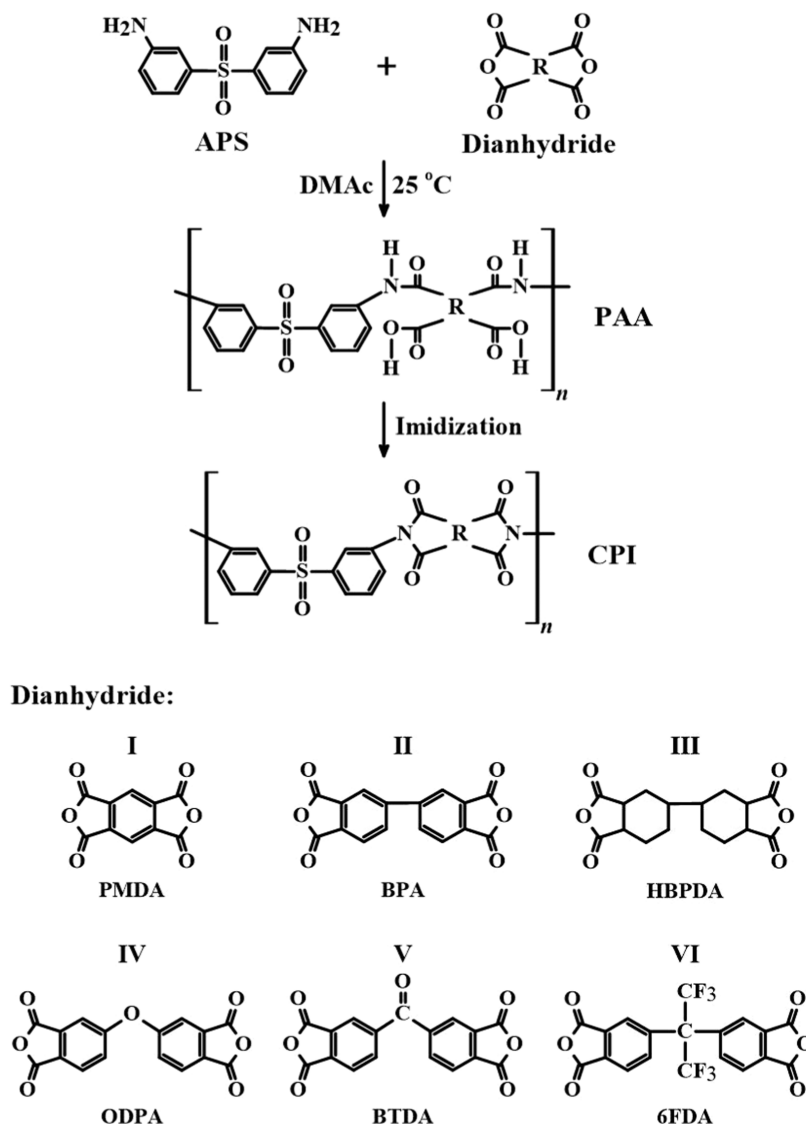
parency compared to aromatic CPI.^{14,15} However, if the CT-complex effect is suppressed, the movement of π electrons in the main chain is hindered, and while the optical properties increase, the thermal and mechanical properties decrease because the attraction and resonance effects acting between chains are lowered.^{16–18}

Glass-based electronic materials have been used widely for several years. Among them, flexible and transparent indium–tin–oxide (ITO) glass is conductive and has been used in the fields of display substrates, microelectronics, and electrical and optoelectronic engineering.^{19–21} However, using ITO glass as a general-purpose electronic material is difficult because of the scarcity and high cost of indium.^{22–24} Additionally, glass is difficult to process because it is heavy, brittle, and sensitive to rapid temperature changes and may be damaged during deposition processes performed at high temperatures.²⁵ Although CPI has a low yield, mass-production methods have been developed to some extent, and it can replace glass in display electronic materials because of its high light transmittance and excellent thermodynamic properties. CPI can

Received: January 5, 2024
Revised: February 7, 2024
Accepted: February 14, 2024
Published: February 27, 2024



Scheme 1. Synthetic Routes of CPI Films Based on APS Diamine



also be used as inexpensive and highly productive polymer films with various properties by selecting an appropriate monomer structure.^{24,26}

Recently, CPI has been widely used as an integrated material for semiconductor materials such as liquid crystal display (LCD) and plasma display panel (PDP) because of the lightweight and precision of electronic products.²⁷ In addition, much research is being conducted on the use of CPI as a light and flexible plastic substrate for displays, which can act as a substitute for glass. Therefore, CPI is not only an excellent polymer material that can replace glass but can also be fully utilized in future electronic materials such as wearable and rollable electronic devices.^{28–30}

Until now, most monomers used to maximize the properties of CPI were mainly composed of benzene or equivalent aromatic structures. However, benzene-based CPI polymers have low solubility for processing because of their rigid aromatic structure and strong attraction between the main chains; therefore, they are processed only through heat treatment in the poly(amic acid) (PAA) state. Therefore, to date, research on CPI synthesis has focused on improving the solubility and processability without significantly reducing the

heat resistance in a fully imidized state by changing the chemical structure through the use of various monomers.³¹ For this purpose, various studies have been conducted on amide imides, ether imides, and sulfone imides, which contain functional groups such as amide, ether, and sulfone, respectively, showing high heat resistance and mechanical properties.^{32–34} Additionally, the optical transparency and solubility have been improved by using monomers with an alicyclic structure.^{35,36}

CPI samples were synthesized by reacting bis(3-amino-phenyl) sulfone (APS) diamine with six dianhydrides. The six dianhydrides used for CPI synthesis were pyromellitic dianhydride (PMDA), 4,4'-bipthalic anhydride (BPA), dicyclohexyl-3,4,3',4'-tetracarboxylic dianhydride (HBPDA), 4,4'-oxydiphthalic anhydride (ODPA), 3,3',4,4'-benzophenonetetracarboxylic dianhydride (BTDA), and 4,4'-(hexafluoroisopropylidene)diphthalic anhydride (6FDA). These dianhydrides mainly contain a bent *meta* (*m*)-structure, an ether or ketone functional group on the main chain, a bulky hexafluoropropyl substituent, or a cyclohexyl alicyclic moiety, which are structures likely to exhibit the properties of CPI.

The thermomechanical properties, optical transparency, and solubility of CPI films obtained from the six different dianhydride monomers were investigated, and the correlation between the structure of the monomers and the physical properties of the CPI was explained. Simultaneously, the CPI results obtained for different monomers were compared.

The purpose of this study was to synthesize new CPIs, establish the conditions for CPI formation through the correlation between the monomer structure and CPI physical properties, and investigate the physical properties of CPIs using alicyclic monomers that have not been used frequently.

2. RESULTS AND DISCUSSION

2.1. FT-IR and ^{13}C NMR Analyses. CPIs were synthesized using the same diamine, APS, and six different dianhydrides (Scheme 1), and the FT-IR results are shown in Figure 1. The

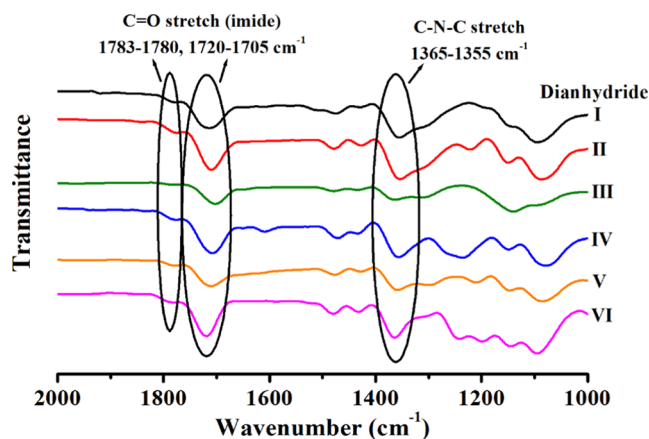


Figure 1. FT-IR spectra of the CPI film based on APS diamine.

actual FT-IR scan range was 4000–1000 cm^{-1} , but no peaks were observed from 4000 to 2000 cm^{-1} , so only 2000–1000 cm^{-1} is shown in Figure 1. C=O stretching peaks were observed in the ranges of 1783–1780 and 1720–1705 cm^{-1} . In particular, a characteristic peak corresponding to C–N–C stretching observed in the imide functional group was identified in the range of 1365–1355 cm^{-1} , confirming that six types of CPIs were synthesized.³⁷

The chemical structures of the synthesized CPIs were confirmed not only by FT-IR but also by ^{13}C NMR. Only the results for structures I and IV were obtained, as shown in Figures 2 and S1, because all of the dianhydride monomer structures were the same. Structure I was analyzed as follows: Peaks *a* and *c* corresponding to the carbon atoms of benzene in dianhydride appeared at 122.94 and 139.53 ppm, and carbon *e* in the anhydride was observed at 168.12 ppm. Additionally, carbons *b* and *d* of benzene included in the diamine were found at 133.41 and 145.17 ppm. The rotating sideband marked with an asterisk (*) indicates the sideband of peak *b*. The chemical shifts for each peak of structure IV are summarized in Table S1. The chemical shifts of all of the carbon atoms obtained from ^{13}C NMR were consistent with the synthesized chemical structures.³⁸ Therefore, the successful synthesis of CPI was confirmed by FT-IR and ^{13}C NMR results.

2.2. Thermal Properties. As CPI is mostly an amorphous polymer, the melt transition temperature cannot be observed using differential scanning calorimetry (DSC), and the thermal

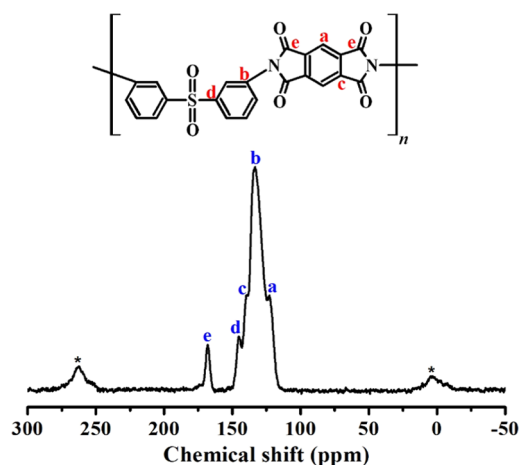


Figure 2. ^{13}C MAS NMR spectrum of the CPI film obtained by the reaction of APS with PMDA (structure I).

properties of CPI are mainly explained by the glass transition temperature (T_g). The T_g not only varies depending on the structure of the monomers that make up the polymer but is also affected by the type of substituent, free volume due to chain movement, secondary bonds such as hydrogen bonds within the main chain, and curing reaction.^{39,40} In the case of composite materials, the T_g is directly affected by dispersed fillers.^{41–43} Additionally, the T_g is affected by the stiffness and flexibility of the polymer chains and is thus greatly affected by the degree of chain interaction and segmental motion resulting from free volume changes.⁴⁴ Table 1 summarizes the T_g values

Table 1. Thermal Properties of CPI Films Based on APS Diamine

dianhydride	LV. ^a (dL/g)	T_g (°C)	T_D^{ib} (°C)	wt _R ^{600c} (%)	CTE ^d (ppm/°C)
I	0.91	251	455	69	40
II	insoluble	244	464	76	39
III	0.67	209	442	26	56
IV	0.61	213	460	71	50
V	insoluble	223	471	73	50
VI	0.83	225	460	69	53

^aInherent viscosity was measured at a concentration of 0.1 dL/g solution at 25 °C. ^bInitial decomposition temperature at 2% weight loss. ^cWeight percent of residue at 600 °C. ^dCTE was measured between 50 and 200 °C.

of CPIs composed of various monomers. The T_g values of CPIs synthesized from various monomer structures were in the range of 209–251 °C. To reveal the correlation between the monomer structure and physical properties of the synthesized CPI film, several three-dimensional polymer structures are shown in Figure 3.

Structure I, containing PMDA in Figure 3, showed the highest T_g value ($T_g = 251$ °C) because it contained only benzene and was the simplest linear structure among the six monomer structures. Structure II containing BPA is completely *m*-structured and contains a very rigid biphenyl monomer structure; therefore, segmental motion is very difficult compared to that of other structures, resulting in the highest T_g (244 °C). On the other hand, structure III containing HBPDA is completely *m*-structured but contains an alicyclic cyclohexane monomer structure; thus, it exhibits the lowest T_g

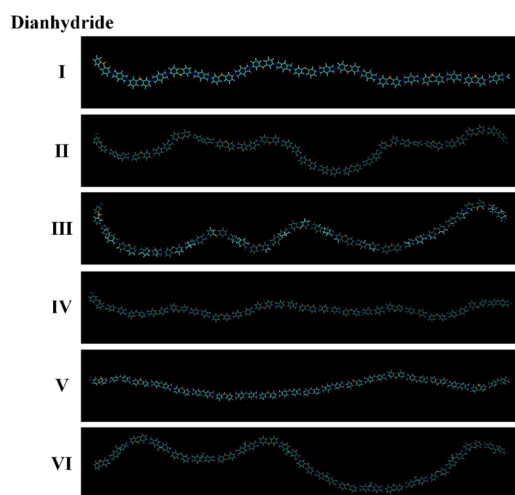


Figure 3. 3D Chemical structures of CPI films based on APS diamine.

(209 °C) due to easier segmental movement at lower temperatures than the other structures.⁴⁵ Structure IV showed a low T_g (213 °C) because it was free to rotate around the central ether bond, and the segmental motion was not hindered. Structures V and VI showed higher T_g values than structure IV owing to free volume effects and difficulty in achieving segmental motion due to the larger substituents. This is probably because the bulky C=O and $-\text{CF}_3$ groups inhibit the segmental motion of the chain and increase the thermal energy required for chain motion. The T_g values of structures V and VI were 223 and 226 °C, respectively. Figure 4 shows the DSC thermograms of CPI films obtained by using various monomer structures.

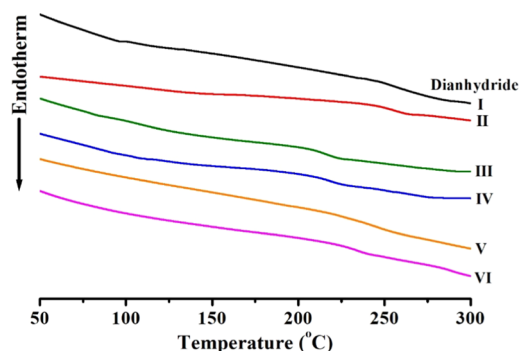


Figure 4. DSC thermograms of CPI films based on APS diamine.

Thermogravimetric analysis (TGA) thermograms are shown in Figure 5, and the initial decomposition temperature (T_D^i) and residual weight at 600 °C (wt_R^{600}) are presented in Table 1. For each structure, T_D^i was in the range of 442–471 °C. Structure III showed a low T_D^i owing to its poor molecular stacking between the polymer chains and weak intermolecular attraction due to their bent shapes. In particular, this structure exhibited the lowest T_D^i at 442 °C because it had an alicyclic moiety with low thermal stability. In contrast, linear structures IV and V showed relatively high thermal stabilities (460 and 471 °C) because the linear molecular chain structure allows molecular bonding between the main polymer chains through excellent molecular stacking^{46,47} (see Figure 3). Despite its bent chain shape, structure VI exhibited a high T_D^i (460 °C)

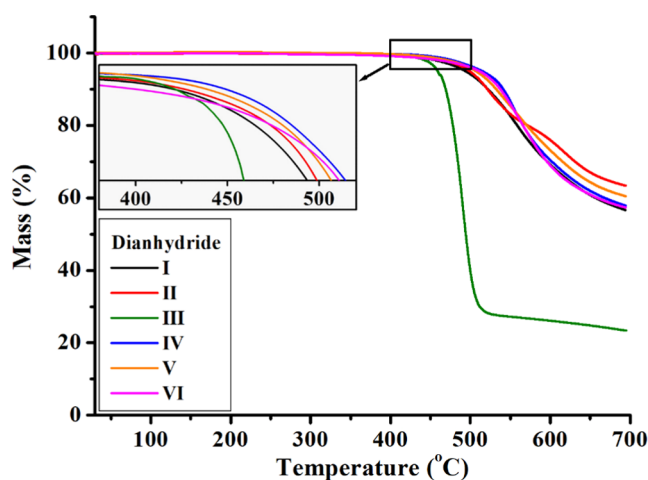


Figure 5. TGA thermograms of CPI films based on APS diamine.

due to the presence of the thermally stable $-\text{CF}_3$ substituent (see Table 1).

The percentage of residues heated to 600 °C (wt_R^{600}) values of all CPI structures except structure III generally showed high values of 69–76%. As previously explained, structure III containing an alicyclic cyclohexane moiety with a low thermal stability showed the lowest value of 26%.

The coefficient of thermal expansion (CTE) is defined as the change in the segment length per unit temperature increase. When polymers are heated, they relax in the direction perpendicular to the main chain. However, if the main chain of the polymer has an aromatic structure with high thermal stability or the entire polymer chain is rigid and straight, heat transfer is hindered, and expansion does not occur easily.^{48,49} Structure I is a rigid rod-type straight *para*-structure that is difficult to change with heat treatment. In addition, although structure II has an *m*-structure, it has excellent dimensional resistance because it contains a rigid biphenyl moiety and exhibits high thermal stability. Structures I and II showed relatively low CTE values of 39–40 ppm/°C. However, the highest CTE value was observed for structure III because it contained an alicyclic moiety with very low thermal stability, and the overall chain structure was bent (56 ppm/°C).⁵⁰ Structures IV and V showed CTE values of 50 ppm/°C because the overall chains were straight, and structure VI showed a CTE value of 53 ppm/°C due to the flexible hexafluoropropyl substituent. Figure 6 shows the thermomechanical analysis (TMA) thermograms of CPI with each monomer structure.

2.3. Mechanical Tensile Properties. A universal testing machine (UTM) was used to measure the ultimate tensile strength, initial modulus, and elongation at break (EB) of the CPI films. The mechanical tensile properties obtained using the UTM are listed in Table 2.

The ultimate tensile strengths of structures I and II, which only consist of aromatic benzene moieties in the main chain, were relatively better than those of structures IV–VI, which contain functional groups and flexible substituents.^{51,52} That is, the ultimate strengths of structures I and II were 106 and 119 MPa, respectively. In particular, structure II exhibited a higher value (119 MPa) than structure I because of the greater number of benzene units per monomer repeating unit. However, structure III exhibited the lowest ultimate strength (48 MPa) because the main chain consisted of an alicyclic

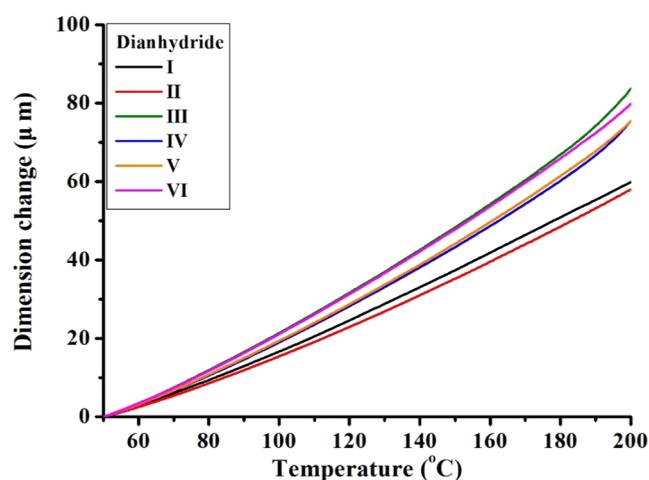


Figure 6. TMA thermograms of CPI films based on APS diamine.

Table 2. Mechanical Properties of CPI Films Based on APS Diamine

dianhydride	ult. str. ^a (MPa)	ini. mod. ^b (GPa)	E.B. ^c (%)
I	106	2.91	5
II	119	3.54	5
III	48	2.79	3
IV	98	3.16	4
V	92	4.40	3
VI	55	3.64	3

^aUltimate strength. ^bInitial modulus. ^cElongation at break.

moiety that was mechanically unstable. Structures IV and V, which contained ether and ketone functional groups, had values of 98 and 92 MPa, respectively. However, structure VI exhibited a low value (55 MPa) because it contained a flexible, bulky hexafluoropropyl group in its main chain.

The initial modulus is proportional to the rigidity of the polymer chain and therefore depends on the presence of rigid rod-shaped benzene in the structure.⁵³ According to the 3D structure in Figure 3, structure V appears to be more linear than the other structures. The shapes of these structures were directly related to their initial moduli (Figure 3). The initial modulus of linear structure V (4.40 GPa) was higher than that of the bent structure, and as already explained in the ultimate strength section, the value of structure III was the lowest (2.79 GPa) because of its flexible structure.

In particular, structures I and II showed better ultimate strengths than structures III–VI, and structure V showed the highest initial modulus value. These excellent mechanical properties are attributed to the shorter length of the repeating monomer units, close chain packing without functional groups or substituents, and attractive forces between the chains of the CPI structure. The EB value of each structure was constant (approximately 3–5%) without significant differences, regardless of the monomer structure.

2.4. Optical Transparency. To investigate the optical transparency of the CPIs, the cut-off wavelength representing the initial transmittance (λ_0), the transmittance at a wavelength of 500 nm (500 nm^{trans}), and YI representing the yellowness index were measured. Optical characterization using UV–vis. spectroscopy is shown in Figure 7, and the results are summarized in Table 3.

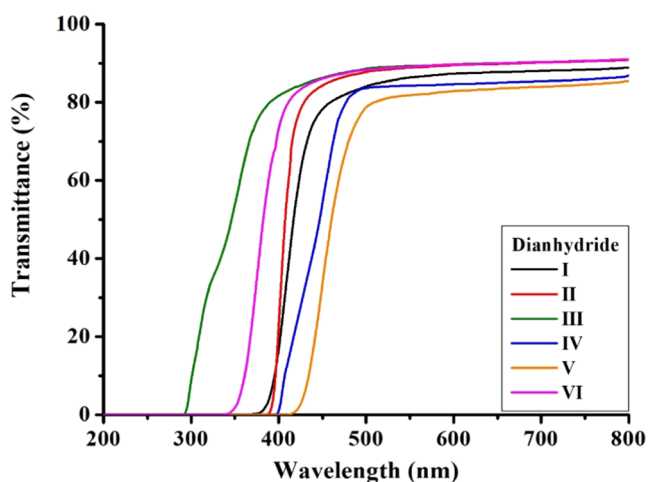


Figure 7. UV–vis. transmittance (%) of CPI films based on APS diamine.

Table 3. Optical Transparencies of CPI Films Based on APS Diamine

dianhydride	thickness ^a (μm)	λ_0 ^b (nm)	500 nm ^{trans} (%)	YI ^c
I	17	371	84	6
II	16	371	87	2
III	17	291	88	1
IV	17	397	83	16
V	18	411	79	23
VI	17	339	88	2

^aFilm thickness. ^bCut-off wavelength. ^cYellow index.

The λ_0 values of all CPI films ranged from 291 to 411 nm depending on the type of monomer, and most light transmissions began before the visible light region. In particular, structure V showed the highest λ_0 value of 411 nm due to its nearly straight linear structure where the CT-complex can occur most easily (Figure 3). However, structure III showed the lowest λ_0 value of 291 nm because it is the structure in which CT-complex formation between the molecular chains is the most difficult because of the bent alicyclic structure. The transmittance at 500 nm was nearly 79–88%, regardless of the dianhydride monomer structure. This excellent transmittance is due to the introduction of functional groups and substituents into the bent monomer, which interfere with the CT-complex effect in the main chain.

The YI can be obtained using the following formula (ASTM E313-96, DIN 6167):

$$YI = 100 \times (aX - bZ) / Y$$

Here, a and b are red and yellow values, respectively, and X , Y , and Z represent the tristimulus values.⁵⁴

The YI values are listed in Table 3. All CPI structures, except for IV and V, exhibited colorless and transparent optical properties, and the YIs were mostly in the range of 1–6.

In particular, structures II, III, and VI showed very low YI values (1 and 2, respectively) compared to the other structures. In addition, structure III not only hindered effective chain packing because of the overall bent m -structure but also showed the lowest YI value compared to the other structures due to its composition of alicyclic monomers. In addition, the reason why structure VI shows a low YI value is because the strong electron-withdrawing group ($-\text{CF}_3$) contained in the

main chain hinders the free movement of π electrons and reduces the CT-complex effect.^{55,56} Meanwhile, structure V showed the highest YI value of 23 because it is a straight linear structure in which CT-complex formation between chains is easily possible (Figure 3). Compared to the straight structure V, structure IV was a more curved structure that made CT-complex formation difficult; therefore, a brighter color (YI = 16) was observed for structure IV than for structure V.

To observe the visual effect, images of CPI films synthesized by using various monomer structures are shown in Figure 8.



Figure 8. Photographs of CPI films based on APS diamine.

Although differences in the color of the films existed depending on the type of dianhydride monomer, there was no significant difference between all of the films. The differences in the color of the films were explained by the YI values.

2.5. Solubility. CPI materials are superengineered polymers with excellent chemical resistance. However, because most polymer main chains consist of a linear structure, they are difficult to dissolve in strong solvents and melt at high temperatures.^{57,58} Therefore, the application of CPI as a superengineering polymer is very limited despite its excellent chemical properties. When processing a CPI solution into a film, selecting an appropriate solvent to increase the solubility to facilitate the process and improve the quality of the film is very important.^{59,60} The solubilities of the six synthesized CPI films measured in various solvents are summarized in Table 4. All CPI films were completely insoluble in general-purpose solvents, such as acetone, chloroform, ethyl alcohol, and methyl alcohol. However, the solubility was particularly high in *N,N'*-dimethylacetamide (DMAc), dimethylformamide

(DMF), and dimethyl sulfoxide (DMSO) and good in *N*-methyl-2-pyrrolidone (NMP) and toluene. In addition, weak solubility was observed in methylene chloride, whereas some CPIs did not dissolve at all. In conclusion, the synthesized CPI films were not soluble in general-purpose solvents but showed excellent solubility in polar solvents.

Structures I and II showed the lowest solubility owing to their simple and highly chemically resistant benzene structures. Structure V exhibited poor solubility because the solvent cannot penetrate, owing to the overall straight main chain shape, as shown in Figure 3. In contrast, structure III showed the highest solubility owing to its highly soluble alicyclic structure, whereas structures IV and VI showed good solubility because of easy attraction and penetration with the solvent owing to the functional group and bulky hexafluoropropyl substituent contained in the chain, respectively.^{61,62} These structural details are consistent with the previously described thermomechanical properties and can be explained using the 3D polymer structure shown in Figure 3.

3. CONCLUSIONS

In this study, APS diamine was used to synthesize PAA with an overall *m*-substituted structure by reacting it with six different dianhydride monomers containing $-O-$ and $-C=O$ functional groups and $-CF_3$ substituents. PAA fabricated CPI films with new structures through a step-by-step heat treatment. The thermomechanical and optical properties and solubility of the synthesized CPIs varied depending on the monomer structure of the dianhydride. CPI films composed of only benzene dianhydride monomers had excellent thermomechanical properties. Conversely, CPI films containing functional groups, substituents, and alicyclic moieties show excellent optical transparency and easy solubility. When the overall shape of the polymer chain was bent, the optical transparency was superior to that of a straight chain, and the YI values were in the range of 1–2.

The newly synthesized CPI films exhibited the characteristics of a superengineered polymer and therefore can be used in flexible display films, solar panel substrates, and rollable and wearable devices that require excellent thermomechanical properties and optical transparency. If an appropriate monomer structure is selected, CPI is a promising polymer material that can replace glass, which has been widely used in various electronic materials for a long time.

4. EXPERIMENTAL METHOD

4.1. Materials. Six dianhydride monomers, including APS, were purchased from TCI (Tokyo, Japan). DMAc, purchased from Sigma-Aldrich (Yongin, Korea), was used to completely remove moisture using a molecular sieve. All of the solvents

Table 4. Solubility Tests of CPI Films Based on APS Diamine^a

dianhydride	Act	CHCl ₃	CH ₂ Cl ₂	DMAc	DMF	DMSO	MeOH	EtOH	NMP	Py	THF	Tol
I	×	×	×	○	○	⊙	×	×	△	△	△	○
II	×	×	×	×	×	×	×	×	△	×	×	×
III	△	○	△	⊙	⊙	⊙	×	×	△	○	△	⊙
IV	×	×	×	⊙	⊙	○	×	×	⊙	△	×	×
V	×	×	×	×	△	×	×	×	×	△	×	×
VI	△	×	⊙	⊙	⊙	⊙	×	×	○	△	○	×

^a⊙: excellent, ○: good, △: poor, ×: very poor. Act: Acetone, DMAc: *N,N*-dimethylacetamide, DMF: *N,N*-dimethylformamide, DMSO: dimethyl sulfoxide, NMP: *N*-methyl-2-pyrrolidone, Py: Pyridine, THF: tetrahydrofuran, Tol: Toluene.

used for the solubility measurements were used without purification.

4.2. Synthesis of CPI Films. The route for the synthesis of PAAs and CPIs via the reaction of various diamine monomers with APS is summarized in [Scheme 1](#). Although the monomer structures are different, the CPI synthetic method is the same; therefore, only the synthesis using PMDA (I) is described. APS (3.23 g, 1.30×10^{-2} mol) was added to 12 mL of DMAc and completely dissolved by stirring. Then, PMDA (2.83 g, 1.30×10^{-2} mol) was added to the APS solution. This solution was stirred under a nitrogen stream for 1 h at 0 °C and 14 h at room temperature, respectively, to obtain a PAA solution. The obtained PAA solution was poured evenly onto a glass plate and stabilized in a 50 °C vacuum oven for 2 h. The solvent was completely removed by holding the solution under vacuum at 80 °C for 1 h. For the complete imide reaction, PAA was heated under an N₂ atmosphere at various heat treatment conditions. The heat treatment conditions for each stage are listed in detail in [Table 5](#). The heat-treated CPI film was

Table 5. Heat Treatment Conditions of the CPI Films Based on APS Diamine

sample	temperature (°C)/time (h)/pressure (Torr)
PAA	0/1/760 → 25/14/760 → 50/2/1 → 80/1/1
CPI I	110/0.5/1 → 140/0.5/1 → 170/0.5/1 → 195/0.8/1 → 220/0.8/1 → 235/2/1
CPI II	110/0.5/1 → 140/0.5/1 → 170/0.5/1 → 195/2/1 → 220/4/1 → 235/6/1 → 250/2/1
CPI III	110/0.5/1 → 140/0.5/1 → 170/0.5/1 → 195/0.8/1 → 220/0.8/1 → 235/2/1 → 250/2/1
CPI IV	110/0.5/1 → 140/0.5/1 → 170/0.5/1 → 195/0.8/1 → 220/0.8/1 → 235/2/1 → 250/2/1
CPI V	110/0.5/1 → 140/0.5/1 → 170/0.5/1 → 195/0.8/1 → 220/0.8/1 → 235/2/1 → 250/2/1
CPI VI	110/0.5/1 → 140/0.5/1 → 170/0.5/1 → 195/0.8/1 → 220/0.8/1 → 235/2/1 → 250/2/1

separated from the glass plate in a 5 wt % hydrofluoric acid aqueous solution. To increase the reliability of the results, the obtained CPI films were synthesized to have a constant thickness of 16–18 μm. All of the films obtained had a size of approximately 10 × 10 cm². Except for the CPIs formed using BPA and BTDA, the inherent viscosities of all of the CPI films were measured by dissolving them in DMAc, and the viscosity values were in the range 0.61–0.91 dL/g (see [Table 1](#)).

4.3. Characterization. To confirm the structures of various CPIs, FT-IR (PerkinElmer, L-300, London, U.K.) and solid-state ¹³C CP/MAS NMR (Bruker, 400 DSX, Berlin, Germany) were used.

DSC (F3200 Netzsch, Munchen, Germany) and TGA (TA Q-500, New Castle, New Castle, NJ) were used to investigate the thermal properties of the CPI films. All experiments were performed under N₂ atmosphere, and the heating scan rate was 20 °C/min. TMA (Seiko, TMA/SS100, Tokyo, Japan) was used to determine the CTE. CTE values were obtained in the range of 50–200 °C by increasing the temperature at 5 °C/min with a load of 0.1 N through secondary heating.

Mechanical properties were measured using a UTM instrument (Shimadzu, JP/AG-50KNX, Tokyo, Japan) at a crosshead speed of 5 mm/min. Each sample was measured at least 10 times, and the average value was calculated within the error range. The experimental errors of the ultimate strength and initial modulus were within ±1 MPa and ±0.05 GPa, respectively.

The light transmittance at a specific wavelength and YI were measured using a UV–vis spectrometer (Shimadzu, UV-3600,

Tokyo, Japan) and a spectrophotometer (Konica Minolta, CM-3600d, Tokyo, Japan), respectively.

■ ASSOCIATED CONTENT

Supporting Information

The Supporting Information is available free of charge at <https://pubs.acs.org/doi/10.1021/acsomega.4c00175>.

¹³C NMR spectrum of the CPI film and the corresponding chemical shift of APS with ODP. (PDF).

■ AUTHOR INFORMATION

Corresponding Author

Jin-Hae Chang – Institute of Carbon Technology, Jeonju University, Jeonju 55069, Korea; orcid.org/0000-0002-7323-9042; Email: jhchang@jj.ac.kr

Authors

Yeji Na – Graduate School of Carbon Convergence Engineering, Jeonju University, Jeonju 55069, Korea

Sungsoo Kang – Graduate School of Carbon Convergence Engineering, Jeonju University, Jeonju 55069, Korea

Lee Ku Kwac – Graduate School of Carbon Convergence Engineering, Jeonju University, Jeonju 55069, Korea; Institute of Carbon Technology, Jeonju University, Jeonju 55069, Korea

Hong Gun Kim – Institute of Carbon Technology, Jeonju University, Jeonju 55069, Korea

Complete contact information is available at:

<https://pubs.acs.org/doi/10.1021/acsomega.4c00175>

Author Contributions

J.-H.C. designed the project and wrote the manuscript. S.K., L.K.K., and H.G.K. reviewed and data analyzed. Y.N. prepared the samples and participated in the data analysis. All authors have read and agreed to the published version of the manuscript.

Notes

The authors declare no competing financial interest.

■ ACKNOWLEDGMENTS

This research was supported by the Basic Science Research Program through the National Research Foundation of Korea (NRF) funded by the Ministry of Education (2016R1A6A1A03012069). This work also was supported by the National Research Foundation of Korea (NRF) grant funded by the Korea Government (MSIT) (2022R1A2C1009863).

■ REFERENCES

- Feng, C. P.; Bai, L.; Bao, R.-Y.; Wang, S.-W.; Liu, Z.; Yang, M.-B.; Chen, J.; Yang, W. Superior thermal interface materials for thermal management. *Compos. Commun.* **2019**, *12*, 80–85.
- Dasgupta, B.; Sen, S. K.; Banerjee, S. Gas transport properties of fluorinated poly(ether imide) membranes containing indan moiety in the main chain. *J. Membr. Sci.* **2009**, *345*, 249–256.
- Lee, D.; Lim, Y.-W.; Im, H.-G.; Jeong, S.; Ji, S.; Kim, Y. H.; Choi, G.-M.; Park, J.-U.; Lee, J.-Y.; Jin, J.; Bae, B.-S. Bioinspired transparent laminated composite film for flexible green optoelectronics. *ACS Appl. Mater. Interfaces* **2017**, *9*, 24161–24168.
- Ghosh, S.; Banerjee, S. 9-Alkylated fluorene-based poly(ether imide)s and their gas transport properties. *J. Membr. Sci.* **2016**, *497*, 172–182.

- (5) Liaw, D.-J.; Wang, K.-L.; Huang, Y.-C.; Lee, K.-R.; Lai, J.-Y.; Ha, C.-S. Advanced polyimide materials: Syntheses, physical properties and applications. *Prog. Polym. Sci.* **2012**, *37*, 907–974.
- (6) Chatterjee, R.; Bisoi, S.; Kumar, A. G.; Padmanabhan, V.; Banerjee, S. Polyimides containing phosphaphenanthrene skeleton: gas transport properties and molecular dynamics simulations. *ACS Omega* **2018**, *3*, 13510–13523.
- (7) Banerjee, S.; Madhra, M. K.; Kute, V. Polyimides 6: Synthesis, characterization, and comparison of properties of novel fluorinated poly(ether imides). *J. Appl. Polym. Sci.* **2004**, *93*, 821–832.
- (8) Dasgupta, B.; Banerjee, S. A study of gas transport properties of semifluorinated poly(ether imide) membranes containing cardo diphenylfluorene moieties. *J. Membr. Sci.* **2010**, *362*, 58–67.
- (9) Chen, C.-J.; Yen, H.-J.; Hu, Y.-C.; Liou, G.-S. Novel programmable functional polyimides: Preparation, mechanism of CT induced memory, and ambipolar electrochromic behavior. *J. Mater. Chem. C* **2013**, *1*, 7623–7634.
- (10) Nishihara, M.; Christiani, L.; Staykov, A.; Sasaki, K. Experimental and theoretical study of charge-transfer complex hybrid polyimide membranes. *J. Polym. Sci., Part B: Polym. Phys.* **2014**, *52*, 293–298.
- (11) Chang, C.-W.; Yen, H.-J.; Huang, K.-Y.; Yeh, J.-M.; Liou, G.-S. Novel organosoluble aromatic polyimides bearing pendant methoxy-substituted triphenylamine moieties: synthesis, electrochromic, and gas separation properties. *J. Polym. Sci., Part A: Polym. Chem.* **2008**, *46*, 7937–7949.
- (12) Hasegawa, M.; Hoshino, Y.; Katsura, N.; Ishii, J. Superheat-resistant polymers with low coefficients of thermal expansion. *Polymer* **2017**, *111*, 91–102.
- (13) Ni, H.-J.; Liu, J.-G.; Wang, Z.-H.; Yang, S.-Y. A review on colorless and optically transparent polyimide films: Chemistry, process and engineering applications. *J. Ind. Eng. Chem.* **2015**, *28*, 16–27.
- (14) Matsumoto, T.; Mikami, D.; Hashimoto, T.; Kaise, M.; Takahashi, R.; Kawabata, S. Alicyclic polyimides – a colorless and thermally stable polymer for opto-electronic devices. *J. Phys.: Conf. Ser.* **2009**, *187*, 012005.
- (15) Jeon, H.; Kwac, L. K.; Kim, H. G.; Chang, J.-H. Comparison of properties of colorless and transparent polyimide films using various diamine monomers. *Rev. Adv. Mater. Sci.* **2022**, *61*, 394–404.
- (16) Liu, J.-G.; Nakamura, Y.; Shibasaki, Y.; Ando, S.; Ueda, M. High refractive index polyimides derived from 2,7-bis(4-aminophenylsulfanyl)thianthrene and aromatic dianhydrides. *Macromolecules* **2007**, *40*, 4614–4620.
- (17) Kim, Y. N.; Lee, J.; Kim, Y.-O.; Kim, J.; Han, H.; Jung, Y. C. Colorless polyimides with excellent optical transparency and self-healing properties based on multi-exchange dynamic network. *Appl. Mater. Today* **2021**, *25*, 101226.
- (18) Choi, I. H.; Chang, J.-H. Colorless polyimide nanocomposite films containing hexafluoroisopropylidene group. *Polym. Adv. Technol.* **2011**, *22*, 682–689.
- (19) Shen, Y.; Feng, Z.; Zhang, H. Study of indium tin oxide films deposited on colorless polyimide film by magnetron sputtering. *Mater. Des.* **2020**, *193*, 108809.
- (20) Lozano, A. E.; Abajo, J. D.; Campa, J. G.; Guillén, C.; Herrero, J.; Gutierrez, M. T. Thin-film polyimide/indium tin oxide composites for photovoltaic applications. *J. Appl. Polym. Sci.* **2007**, *103*, 3491–3497.
- (21) Morikawa, H.; Fujita, M. Crystallization and electrical property change on the annealing of amorphous indium-oxide and indium-tin-oxide thin films. *Thin Solid Films* **2000**, *359*, 61–67.
- (22) Choi, M.-C.; Kim, Y.; Ha, C.-S. Polymers for flexible displays: from material selection to device applications. *Prog. Polym. Sci.* **2008**, *33*, 581–630.
- (23) Kim, J.-H.; Choi, M.-C.; Kim, H.; Kim, Y.; Chang, J.-H.; Han, M.; Kim, I.; Ha, C.-S. Colorless polyimide/organoclay nanocomposite substrates for flexible organic light-emitting devices. *J. Nanosci. Nanotechnol.* **2010**, *10*, 388–396.
- (24) Wang, P. C.; MacDiarmid, A. G. Integration of polymer-dispersed liquid crystal composites with conducting polymer thin films toward the fabrication of flexible display devices. *Displays* **2007**, *28*, 101–104.
- (25) Na, Y.; Kwac, L. K.; Kim, H. G.; Joo, Y. L.; Chang, J.-H. Effects of organoclay on colorless and transparent polyimide nanocomposites: thermomechanical properties, morphology, and optical transparency. *RSC Adv.* **2023**, *13*, 16285–16292.
- (26) Lee, C.; Seo, J.; Shul, Y.; Han, H. Optical properties of polyimide thin films. Effect of chemical structure and morphology. *Polym. J.* **2003**, *35*, 578–585.
- (27) Kim, M.; Park, J.; Ji, S.; Shin, S.-H.; Kim, S.-Y.; Kim, Y.-C.; Kim, J.-Y.; Park, J.-U. Fully-integrated, bezel-less transistor arrays using reversibly foldable interconnects and stretchable origami substrates. *Nanoscale* **2016**, *8*, 9504–9510.
- (28) Jung, Y.; Byun, S.; Park, S.; Lee, H. Polyimide–organosilicate hybrids with improved thermal and optical properties. *ACS Appl. Mater. Interfaces* **2014**, *6*, 6054–6061.
- (29) Xu, H.; Luo, D.; Li, M.; Xu, M.; Zou, J.; Tao, H.; Lan, L.; Wang, L.; Peng, J.; Cao, Y. A flexible AMOLED display on the PEN substrate driven by oxide thin-film transistors using anodized aluminium oxide as dielectric. *J. Mater. Chem. C* **2014**, *2*, 1255–1259.
- (30) Xia, X.; Zhang, S.; He, X.; Zheng, F.; Lu, Q. Molecular necklace strategy for enhancing modulus toughness of colorless transparent polyimides for cover window application. *Polymer* **2022**, *259*, 125358.
- (31) Choi, C. H.; Chang, J.-H. Polyimide films using dianhydride containing ester linkages and various amine monomers. *Polymer* **2013**, *54*, 618–624.
- (32) Liaw, D.-J.; Huaug, C.-C.; Chen, W.-H. Color lightness and highly organosoluble fluorinated polyamides, polyimides and poly-(amide-imide)s based on noncoplanar 2,2'-dimethyl-4,4'-biphenylene units. *Polymer* **2006**, *47*, 2337–2348.
- (33) Vora, R. H. Designing of molecular architecture, synthesis and properties of the next generation of state-of-the-art high-performance thermoplastic fluoro-poly(ether amide)s, (6F-PEA), fluoro-poly(ether amide-imide)s (6F-PEAI), and their co-polymers. *Mater. Sci. Eng., B* **2010**, *168*, 71–84.
- (34) Domańska, U.; Zawadzki, M.; Królikowski, M.; Lewandowska, A. Phase equilibria study of binary and ternary mixtures of {N-octylisoquinolinium bis{(trifluoromethyl)sulfonyl}imide + hydrocarbon, or an alcohol, or water}. *Chem. Eng. J.* **2012**, *181*–182, 63–71.
- (35) Zhai, L.; Yang, S.; Fan, L. Preparation and characterization of highly transparent and colorless semi-aromatic polyimide films derived from alicyclic dianhydride and aromatic diamines. *Polymer* **2012**, *53*, 3529–3539.
- (36) Hu, X.; Mu, H.; Wang, Y.; Wang, Z.; Yan, J. Colorless polyimides derived from isomeric dicyclohexyl-tetracarboxylic dianhydrides for optoelectronic applications. *Polymer* **2018**, *134*, 8–19.
- (37) Pavia, D. L.; Lampman, G. M.; Kriz, G. S.; Vyvyan, J. R. *Introduction to Spectroscopy*; Cengage Learning: Boston, MA, 2008, Chapter 2, pp 14–95.
- (38) Pavia, D. L.; Lampman, G. M.; Kriz, G. S.; Vyvyan, J. R. *Introduction to Spectroscopy*; Cengage Learning: Boston, MA, 2008, Chapter 4, pp 146–183.
- (39) Xie, R.; Weisen, A. R.; Lee, Y.; Aplan, M. A.; Fenton, A. M.; Masucci, A. E.; Kempe, F.; Sommer, M.; Pester, C. W.; Colby, R. H.; Gomez, E. D. Glass transition temperature from the chemical structure of conjugated polymers. *Nat. Commun.* **2020**, *11*, No. 893.
- (40) Lian, M.; Zheng, F.; Lu, X.; Lu, Q. Tuning the heat resistance properties of polyimides by intermolecular interaction strengthening for flexible substrate application. *Polymer* **2019**, *173*, 205–214.
- (41) Agag, T.; Takeichi, T. Polybenzoxazine–montmorillonite hybrid nanocomposites: synthesis and characterization. *Polymer* **2000**, *41*, 7083–7090.
- (42) Ju, J.; Chang, J.-H. Characterizations of poly(ester imide) nanocomposites containing organically modified hectorite. *Macromol. Res.* **2014**, *22*, 549–556.

- (43) Khonakdar, H. A.; Jafari, S. H.; Hässler, R. Glass-transition-temperature depression in chemically crosslinked low-density polyethylene and high-density polyethylene and their blends with ethylene vinyl acetate copolymer. *J. Appl. Polym. Sci.* **2007**, *104*, 1654–1660.
- (44) Yang, S. Y.; Park, C. E.; Jung, M. S. Effects of reactive end-capper on mechanical properties of chemical amplified photosensitive polyimide. *Polymer* **2003**, *44*, 3243–3249.
- (45) Zhuang, Y.; Seong, J. G.; Lee, Y. M. Polyimides containing aliphatic/alicyclic segments in the main chains. *Prog. Polym. Sci.* **2019**, *92*, 35–88.
- (46) Sasaki, T.; Moriuchi, H.; Yano, S.; Yokota, R. High thermal stable thermoplastic–thermosetting polyimide film by use of asymmetric dianhydride (a-BPDA). *Polymer* **2005**, *46*, 6968–6975.
- (47) Lian, M.; Zheng, F.; Wu, Q.; Lu, X.; Lu, Q. Incorporating bis-benzimidazole into polyimide chains for effectively improving thermal resistance and dimensional stability. *Polym. Int.* **2020**, *69*, 93–99.
- (48) Hasegawa, M. Development of solution-processable, optically transparent polyimides with ultra-low linear coefficients of thermal expansion. *Polymers* **2017**, *9*, 520–550.
- (49) Lao, H.; Mushtaq, N.; Chen, G.; Jiang, H.; Jiao, Y.; Zhang, A.; Fang, X. Transparent polyamide-imide films with high T_g and low coefficient of thermal expansion: Design and synthesis. *Polymer* **2020**, *206*, 122889.
- (50) Jiang, G.-L.; Wang, D.-Y.; Du, H.-P.; Wu, X.; Zhang, Y.; Tan, Y.-Y.; Wu, L.; Liu, J.-G.; Zhang, X.-M. Reduced coefficients of linear thermal expansion of colorless and transparent semi-alicyclic polyimide films via incorporation of rigid-rod amide moiety: Preparation and properties. *Polymers* **2020**, *12*, 413–427.
- (51) Jang, W.; Seo, J.; Lee, C.; Paek, S.-H.; Han, H. Residual stress and mechanical properties of polyimide thin films. *J. Appl. Polym. Sci.* **2009**, *113*, 976–983.
- (52) Mi, Z.; Liu, Z.; Yao, J.; Wang, C.; Zhou, C.; Wang, D.; Zhao, X.; Zhou, J.; Zhang, Y.; Chen, C. Transparent and soluble polyimide films from 1,4:3,6-dianhydro-D-mannitol based dianhydride and diamines containing aromatic and semiaromatic units: Preparation, characterization, thermal and mechanical properties. *Polym. Degrad. Stab.* **2018**, *151*, 80–89.
- (53) Saeed, M. B.; Zhan, M.-S. Effects of monomer structure and imidization degree on mechanical properties and viscoelastic behavior of thermoplastic polyimide films. *Eur. Polym. J.* **2006**, *42*, 1844–1854.
- (54) Yang, C.-P.; Su, Y.-Y. Colorless and high organosoluble polyimides from 2,5-bis(3,4-dicarboxyphenoxy)-*t*-butylbenzene dianhydride and aromatic bis(ether amine)s bearing pendent trifluoromethyl groups. *Polymer* **2005**, *46*, 5778–5788.
- (55) Ma, S. L.; Kim, Y. S.; Lee, J. H.; Kim, J. S.; Kim, I.; Won, J. C. Synthesis and properties of colorless polyimide and its nanocomposite for plastic display substrate. *Polymer* **2005**, *29*, 204–210.
- (56) Ghosh, A.; Sen, S. K.; Banerjee, S.; Voit, B. Solubility improvements in aromatic polyimides by macromolecular engineering. *RSC Adv.* **2012**, *2*, 5900–5926.
- (57) Yu, H.-C.; Jung, J.-W.; Choi, J.-Y.; Oh, S. Y.; Chung, C.-M. Structure-property relationship study of partially aliphatic copolyimides for preparation of flexible and transparent polyimide films. *J. Macromol. Sci., Part A* **2017**, *54*, 97–104.
- (58) Yang, C.-Y.; Hsu, L.-C.; Chen, J. S. Synthesis and properties of 6FDA-BisAAF-PPD copolyimides for microelectronic applications. *J. Appl. Polym. Sci.* **2005**, *98*, 2064–2069.
- (59) Ghaemy, M.; Porazizollahy, R.; Bazzar, M. Novel thermal stable organosoluble polyamides and polyimides based on quinoxalin bulky pendent group. *Macromol. Res.* **2011**, *19*, 528–536.
- (60) Kim, M. H.; Hoang, M. H.; Choi, D. H.; Cho, M. J.; Ju, H. K.; Kim, D. W.; Lee, C. J. Electro-optic effect of a soluble nonlinear optical polyimide containing two different chromophores with different sizes in the side chain. *Macromol. Res.* **2011**, *19*, 403–407.
- (61) Yang, C.-P.; Chen, R.-S.; Chen, K.-H. Organosoluble and light-colored fluorinated polyimides based on 2,2-bis[4-(4-amino-2-trifluoromethyl-phenoxy)phenyl]propane and aromatic dianhydrides. *J. Appl. Polym. Sci.* **2005**, *95*, 922–935.
- (62) Maya, E. M.; Lozano, A. E.; Abajo, J.; Campa, J. G. Chemical modification of copolyimides with bulky pendent groups: effect of modification on solubility and thermal stability. *Polym. Degrad. Stab.* **2007**, *92*, 2294–2299.